Design of Strain-Limited Bi-2223 Insert Coils for High-Field Magnets

William Scott Marshall, *Member, IEEE*, Iain Dixon, *Member, IEEE*, and David Larbalestier, *Fellow, IEEE*

***Abstract*—High field solenoid coils made with HTS conductors are limited primarily by total strain and then by critical current. A detailed accounting of all the sources of mechanical strain on a coil is an essential part of the design. Those sources include winding tension, bending about the coil axis, bending to form the layer transition, compression from overbanding, differential thermal contraction, magnetic hoop strain in the radial and axial directions, and thermal expansion from quenches. A design example for a high-field insert coil made with Sumitomo Type HT-NX Bi-2223 conductor is presented, with each of the relevant strains computed explicitly.**

***Index Terms*—Bi-2223, coils, superconducting magnets.**

I. Introduction

For high-field magnet insert coils made with high-temperature superconductors (HTS) operating at 25–30 Tesla, the limiting criterion for operation is the strain acting on the superconductor filaments. Sumitomo Type HT-NX conductor, a filamentary Bi-2223 tape in a silver matrix with nickel alloy laminations, has been shown to be a feasible option for construction of these coils, with demonstrated strain tolerance before degradation exceeding 0.5% in the superconductor filaments.

Bi-2223 offers advantages of commercial availability in 0.3–0.5 km piece lengths, with reduced hysteresis and screening current effects over other options, including REBCO and Bi-2212.

Test articles [1], [2] and coils [3] built by the National High Magnetic Field Laboratory (NHMFL) have successfully demonstrated operation at the sum of winding and hoop strains on the HT-NX conductor filaments above 0.5%.

RIKEN [4] and Tohoku University, with Toshiba [5] have demonstrated successful use of HT-NX in high-field magnet systems. The Bi-2223 insert coils for those magnets were designed to a hoop stress limit. Strain on the superconductor filaments was not reported.

The coil test results in [3] reported the total strain on the outer edge of the conductor, in the nickel alloy laminations above 0.8%. The strain in the superconductor filaments was 0.5%.

Manuscript received October 29, 2018; accepted January 16, 2019. Date of publication February 4, 2019; date of current version March 1, 2019. This work was supported in part by the National Science Foundation (Award DMR-1644779) and in part by the State of Florida. *(Corresponding author: William Scott Marshall.)*

The authors are with the National High Magnetic Field Laboratory, Tallahassee, FL 32310 USA (e-mail: wsmarshall@magnet.fsu.edu).

Color versions of one or more of the figures in this paper are available online at http://ieeexplore.ieee.org

Digital Object Identifier 10.1109/TASC.2019.2897069

TABLE I
Sumitomo Type HT-NX Conductor Properties

Parameter	Value
Bare conductor cross section	4.5 x 0.33 mm
Insulation build	4 x 12.5 micron
Critical current at 77 K, self field	180 A
Critical tensile stress (> 95% Ic retention)	480 MPa
Tensile secant modulus	91 GPa
Critical tensile strain	0.55%

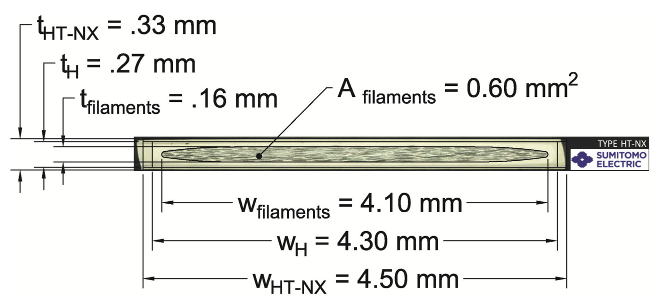

Fig. 1. Cross section of Sumitomo Type HT-NX conductor, with dimensions.

Shen [6] has investigated the added impact of thermal expansion during quench on the conductor strain limit. These findings indicated that the HT-NX conductor tends to fail when the sum of winding, hoop and thermal expansion strains in the conductor filaments during a quench exceeds 0.55%. A relationship between the maximum allowable temperature rise during quench and the sum of winding and hoop strains was observed with sufficient detail to set practical design limits for coils.

The following sections describe the design of an insert coil with HT-NX conductor, with the added consideration for thermal expansion from quench. The impact of reducing the allowable temperature rise to get to higher field is described.

II. High Field Insert Coil Design

A. Conductor Properties

Properties and dimensions used for this design are for the Sumitomo commercial standard Kapton insulated, nickel-alloy laminated Bi-2223 tape, Type HT-NX, and are given in Table I and shown in Fig. 1.

B. Strain-Limited Coil Design

1) Design Assumptions: The conductors are assumed to be self-supporting, so adjacent turns do not bear on one another.

External reinforcement overbanding is not used. The conductor thermal contraction strain is ~0.28%, which is well matched to likely boretube materials such as stainless steel or G-10, and is therefore neglected. Winding tension is < 10 N, which adds $<0.01\%$ to the total strain, and is therefore neglected.

Three dominant sources of coil strain are considered for this design. They include bending strain from winding, magnetic hoop strain, and thermal expansion during a quench. The sum of these terms equals the conductor critical strain, as described in (1).

$$\epsilon_{cr} = \epsilon_{wind}\,(\mathrm{R}) + \epsilon_{hoop}\,(\mathrm{R}) + \epsilon_{quench} \tag{1}$$

2) Critical Strain, ϵ_{cr}: From results reported in [1], [2] and [5], the conductor critical current begins to irreversibly degrade above 0.55%.

3) Bending Strain From Winding: The bending strain, previously described in [3] in terms of the outer surface of the tape, is here described in terms of the outer surface of the conductor filaments.

$$\epsilon_{wind,midplane}\,(R) = \frac{t_{filaments}}{2R} \tag{2a}$$

$$\epsilon_{wind,\,ends}\,(R) = \frac{t_{filaments}}{2R} + \frac{w_{filaments}}{2C\,(R)} \tag{2b}$$

$\epsilon_{wind,midplane}$ is the winding strain in the helical region of the coil winding pack.

$\epsilon_{wind,\,ends}$ is the winding strain at the coil ends, including a term for the curvature of the windings in the 'hard' direction at the layer transition.

$t_{filaments}$ is the thickness of the filament region of the conductor, from Fig. 1, is 0.16 mm.

$w_{filaments}$ is the width of the filament region of the conductor, from Fig. 1, is 4.1 mm.

R is the winding radius of the neutral axis of the conductor.

$C(R)$ is the radius of curvature of the neutral axis of conductor bend in the 'hard' direction at the layer transition.

4) Hoop Strain:

$$\epsilon_{hoop}\,(R, z) = \frac{Bz\,(R, z) \cdot J_{conductor} \cdot R}{E_{secant,conductor}} \tag{3}$$

ϵ_{hoop} is the hoop strain.

$J_{conductor}$ is the conductor current density, defined as the coil current divided by the area cross section of the bare conductor.$E_{secant,conductor}$ is the secant modulus of the conductor. [2]$Bz(R, z)$is the axial component of magnetic field.

5) Thermal Expansion in Quenched Conductor: From Shen [6] an empirical relationship between thermal strain and peak temperature from a quench is derived and is shown in Fig. 2.

ϵ_{quench}, the quench strain, is determined by the design of the protection system and further reduces the allowable maximum operating strain.

6) Design Limits: There is a practical lower limit on the inner radius of the inner coil, because bending strain from winding is inversely proportional to radius, and hoop strain is directly proportional to radius. The winding strain can be the dominant and limiting term if the inner radius is too small.

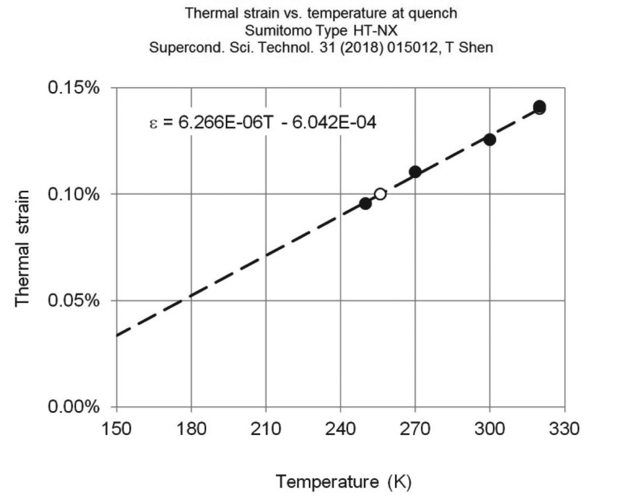

Fig. 2. Thermal strain at quench vs. temperature rise in HT-NX conductor. An extended linear fit to the data is shown with a dashed line. The open circle at 256 K, and 0.10% strain is the design point.

TABLE II
HIGH FIELD INSERT COIL DESIGN

Parameter	Inner coil (Coil 1)	Outer coil (Coil 2)
Inner radius (a1)	44 mm	83 mm
Outer radius (a2)	75 mm	114 mm
Radial turns	86	86
Winding length (2b)	361 mm	425 mm
Axial turns	76	90
Conductor length	2.5 km	4.9 km
Splices [i]	9	17
Current (Iop)	311 A	
Coil current density (Je)	180 A/mm^2	181 A/mm^2
Central field contribution (B0)	6.7 T	6.5 T
Background field	15.0 T	
Total field	28.2 T	

[i] Assuming 300 m piece lengths.

The sum of the location-dependent strains equals the critical strain minus the quench strain.

$$\epsilon_{wind}\,(\mathrm{R}) + \epsilon_{hoop}\,(\mathrm{R}) = \epsilon_{cr} - \epsilon_{quench}\,(T_{max}) \tag{4}$$

For this design, since details of the protection system aren't yet determined, the quench strain is set to 0.1%, which corresponds to a peak temperature of 256 K. The design point is shown as an open circle in Fig. 2. The sum of winding and hoop strains is therefore limited to a maximum value of 0.45%.

C. Insert Coil Design

For this study, the background magnet is the NHMFL 32 T outer coil set, composed of three Nb_3Sn coils, labeled Nb_3Sn 3, 4 and 5 in Fig. 3 and two NbTi sections, labeled NbTi 6 and 7 in Fig. 3, supplied by Oxford Instruments [7], making a central field of 15 T. The two HTS insert coils made with HT-NX conductor are described in Table II and labeled Bi-2223 1 and 2 in Fig. 3.

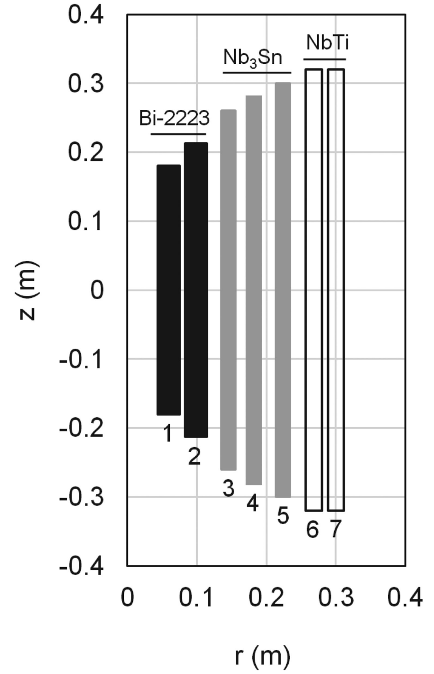

Fig. 3. Half section of coils, drawn to scale. Design details of the Bi-2223 coils 1 and 2, shown in solid black are described in detail. The Nb_3Sn coils 3-5, shown in gray, and NbTi coils 6 and 7, shown in white are described in [7].

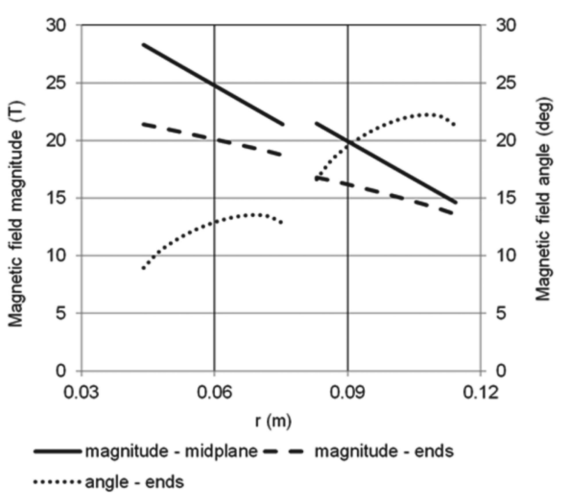

Fig. 4. Magnitude of magnetic field at coil midplane and coil ends, and angle of magnetic field at coil ends. Magnetic field at coil midplane is parallel to coil axis.

1) Magnetic Field on Windings, Critical Current and Operating Fraction: The magnetic field on the windings at the midplane and ends is plotted in Fig. 4.

The critical current and operating fraction of critical current vs. winding radius are graphed at the coil midplane position (z = 0), and at the coil ends (z = b) in Fig. 5. Maximum values are given in Table III.

2) Hoop Stress and Axial Compressive Stress: Magnetic hoop stress vs. coil radius at the coil midplane and ends are graphed in Fig. 6. Hoop stress is the product of the axial component of local magnetic field, current density and winding radius. Maximum values for hoop stress are given in Table III.

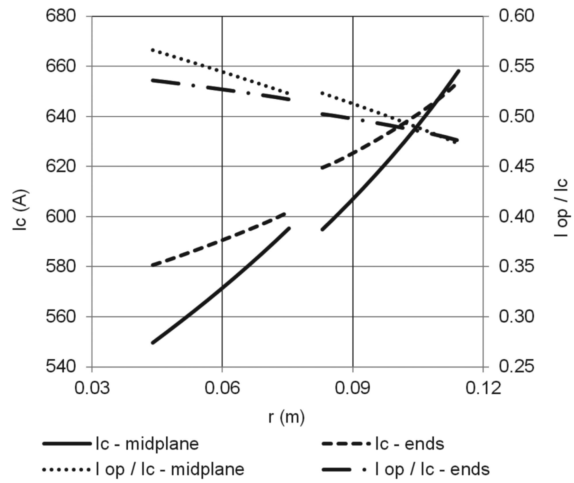

Fig. 5. Critical current and operating fraction of critical current at coil midplane and coil ends vs. winding radius.

TABLE III
FRACTION OF CRITICAL CURRENT, STRESS AND STRAIN

Parameter	Inner coil	Outer coil
Critical current	550 A	595 A
Operating fraction of critical current	0.57	0.52
Maximum hoop stress	325 MPa	262 MPa
Maximum total strain	0.43%	0.45%
Axial force	422 kN	1270 kN
Axial compressive stress	32 MPa	63 MPa
Axial compressive strain	-0.04%	-0.07%

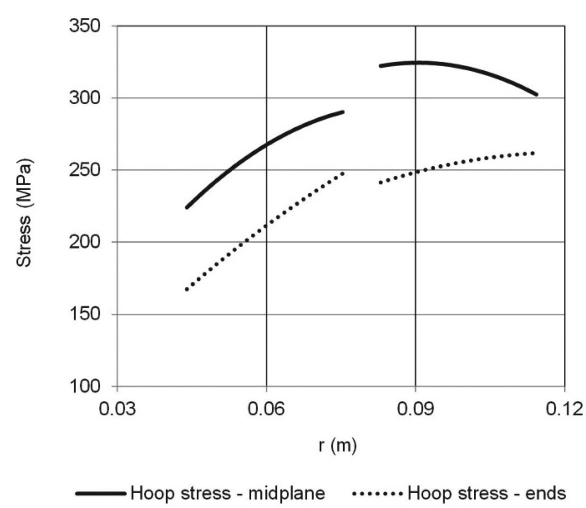

Fig. 6. Hoop stress at coil midplane and coil ends.

Axial compressive stress is:

$$\sigma_z = \frac{F_{axial}}{\pi\left(a_2{}^2 - a_1{}^2\right)} \quad (5)$$

where F_{axial} is the force of two coil halves acting on one another at the coil midplane [8], and $\pi(a_2{}^2 - a_1{}^2)$ is the area of the coil cross section normal to its axis. The result is given in Table III.

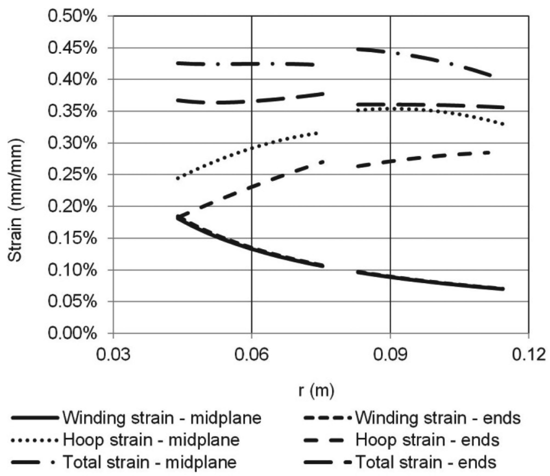

Fig. 7. Winding strain and hoop strain vs. radius at coil midplane and coil ends.

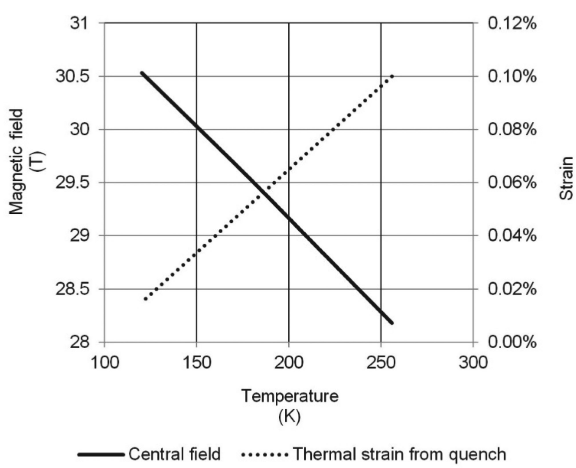

Fig. 8. Maximum central field and thermal strain from quench vs. allowable temperature rise at quench for this coil design.

3) Winding Strain and Hoop Strain: Winding and hoop strains, and their sums for the Bi-2223 coils at the midplane and ends are graphed in Fig. 7. The winding strains at the ends are slightly higher than at the midplane near the inner radius, because of the added strain from the 'hard way' bend at the layer transition, described in Eq. 2b.

4) Quench Temperature: By reducing the allowable peak conductor temperature at quench, the maximum hoop stress allowed during operation is increased, and the HTS coils may be operated safely at a higher current, and make a higher field.

Fig. 8 graphs the impact of reducing the allowable maximum temperature on thermal strain and central magnetic field.

Setting the temperature rise to 256 K limits safe operation of this design to 28.2 T. If the temperature rise can be limited to 120 K, then this magnet may safely operate at 30.5 T.

III. Conclusion

A high field coil design with Sumitomo Type HT-NX conductor is presented, with thermal expansion strain from quench explicitly considered. Safe operation is limited by total strain, including bending, hoop and thermal expansion contributions. Higher field operation is possible if the protection scheme enables a reduction in the peak temperature. The 'self-supporting' assumption makes the analysis of coil stress simple, and therefore useful for iterative design searches. However, finite element or generalized plane strain analysis is needed to fully understand the stress and strain state of the coils.

Acknowledgment

The authors are grateful for the ongoing efforts of M. Bird, E. Arroyo, and M. White of the National High Magnetic Field Laboratory in support of this program.

Thanks to R. Shaw at Sumitomo Electric for his continuing support.

References

[1] W.S. Marshall *et al.*, "Investigation of the strain limit of Sumitomo Type HT-NX conductor and its impact on high field coil design," in *Proc. 8th Workshop on Mech. Electromagn. Properties Composite Supercond.*, Mar. 2016.

[2] A Godeke *et al.*, "A feasibility study of high-strength Bi-2223 conductor for high-field solenoids," *Supercond. Sci. Technol.*, vol. 30, no. 3, 2017, Art. no. 035011.

[3] W.S. Marshall *et al.*, "Fabrication and testing of a Bi-2223 test coil for high field NMR magnets," *IEEE Trans. Appl. Supercond.*, vol. 28, no. 3, Apr. 2018, Art. no. 4301204.

[4] Y. Yanagisawa *et al.*, "Combination of high hoop stress tolerance and a small screening current-induced field for an advanced Bi-2223 conductor coil at 4.2 K in an external field," *Supercond. Sci. Technol.*, vol. 28, no. 12, 2015, Art. no. 125005.

[5] S. Awaji *et al.*, "1st Performance test of the 25 T cryogen-free superconducting magnet," *Supercond. Sci. Technol.*, vol. 30, no. 6, 2017, Art. no. 065001.

[6] T. Shen, L. Ye, and H. Highley, "Strain control of composite superconductors to prevent degradation of superconducting magnets due to a quench: II. High-strength, laminated Ag-sheathed Bi-2223 tapes," *Supercond. Sci. Technol.*, vol. 31, no. 1, 2017, Art. no. 015012.

[7] H.W. Weijers *et al.*, "Progress in the development and construction of a 32-T superconducting magnet," *IEEE Trans. Appl. Supercond.*, vol. 26, no. 4, Jun. 2016, Art. no. 4300807.

[8] Y. Iwasa, *Case Studies in Superconducting Magnets*, 2nd ed. New York, NY, USA: Springer, 2009, pp. 83–97.